J. Condensed Matter Nucl. Sci. 29 (2018) 401–415

Research Article

Statistical Mechanics Models for PdD_x and PdH_x Phase Diagrams with both O-site and T-site Occupation

Peter L. Hagelstein*

Massachusetts Institute of Technology, Cambridge, MA, USA

Abstract

The phase diagram of PdH_x was first understood with the development of statistical mechanics models in the 1930s, where hydrogen atoms were modeled as occupying octahedral sites with an O-site energy that depended on the loading. In an earlier study we made use of a generalization of this kind of model to include both O-site and T-site occupation to model loading in the alpha phase, loading in the beta phase, and to develop a mean field model for the phase diagram of PdH_x. Here we extend the modeling to develop a model phase diagram for PdD_x. Since the PdD_x phase diagram is less studied that the PdH_x phase diagram, the selection of isotherms is an issue, and we encountered minor technical issues in the digitization of published isotherm data. It was possible to develop good extrapolations to low loading (required for our phase diagram optimization), but we found that a reliable extrapolation of isotherms at high temperature to high loading was not possible. Consequently, after some exploration we found that "reasonable" global phase diagram models could be obtained with the introduction of a "guiding" point, where we introduce an estimate for a single pressure at high temperature and high loading to constrain the O-site energies and resulting phase diagram. This underscores the need for experimental measurements in this regime in order to understand the phase diagram. We were successful in optimizing a mean field phase diagram model for PdD_x using this approach. We made use of the isotherms from our earlier modeling for PdH_x to develop a new phase diagram model for PdH_x making use of the same basic approach. The resulting O-site energy curves are qualitatively similar, with a somewhat deeper binding for H at high loading (attributed to the increased lattice expansion), and larger spread in O-site energies as a function of temperature (attributed to the reduced number of configurations accessible at low energy due to the larger excitation energy of the lower mass hydrogen atom).
© 2018 ISCMNS. All rights reserved. ISSN 2227-3123

Keywords: PdD phase diagram, PdH phase diagram, mean-field statistical mechanics model, O-site and T-site occupation of H in Pd, empirical alpha-phase model for PdD_x

1. Introduction

We are interested in the development of a statistical mechanics model for the phase diagram of PdD_x in connection with simulating loading and excess heat in the Fleischmann–Pons experiment [1,2]. Such a model would likely have wider applications; for example, to allow for the estimation of the deuterium chemical potential in PdD_x; to help in the

*E-mail: plh@mit.edu.

© 2018 ISCMNS. All rights reserved. ISSN 2227-3123

development of kinetics models for the deuterium evolution reaction; and to aid in the interpretation of experiments generally involving PdD_x.

What seemed to be a straightforward project at first glance turns quickly into a complicated venture. Where PdH_x has long been studied, PdD_x has received less attention. Where the phase diagram of PdH_x is in reasonable shape, the phase diagram for PdD_x has been less studied. Considerable theoretical work has been devoted to statistical mechanics models for PdH_x, but much less effort has been devoted to the problem of PdD_x.

Early experimental work established that hydrogen isotopes occupy octahedral sites near room temperature. However, it is not possible to model loading in the α-phase of PdH_x or PdD_x accurately over a wide range of temperature based on a statistical mechanics model with only O-site occupation. Instead, models with both O-site and T-site occupation can fit the experimental data [3] very well [4]. Some neutron diffraction experiments show evidence for T-site occupation at higher loading; however, there are also neutron diffraction experiments which do not (see the discussion and references in [5]).

What happens at high loading near room temperature is very much unclear. There are gas loading experiments and electrochemical experiments in which the D/Pd loading ratio is thought to exceed unity [6–8]. Yet there is no agreement within the hydrogen in metals community that palladium is capable of being loaded with H or D above unity under experimentally accessible conditions. And if it is possible for the loading to exceed unity, there is no agreement as to where additional interstitials go, as there are only as many octahedral sites as palladium atoms. One possibility is that double occupation of O-sites occurs. Another is that a phase change occurs with H or D going into T-sites. We have explored models in which T-site occupation occurs when most of the O-sites are filled [9].

A gaping hole in the currently available experimental data sets occurs for high loading and high temperature (it is much easier to measure isotherms near room temperature and at low temperature for high loading). Continuing isotherm measurements at high loading involves high pressure, which becomes problematic at the very high pressures required. As a result, isotherms for PdH_x at elevated temperature simply are not available at high pressure. The isotherm data sets available for PdD_x are less complete than for PdH_x.

In earlier modeling work with PdH_x we made use of empirical extrapolations in an attempt to fill in missing parts of isotherms [10]. At low loading, the extrapolations appear to have worked well. At high loading this was perhaps ill-advised, as there is no reason to believe that the extrapolations used should be accurate.

Another headache is that Pd vacancies are stabilized at high loading, so that phase changes to superabundant vacancy phases are expected. Fukai and Okhuma showed that highly loaded NiH and PdH undergo a phase change where one out of four host metal lattice atoms are missing (after having diffused elsewhere) at elevated temperature [11,12]. A further brief discussion relating to vacancy phases appears in Appendix A. In the models considered here and in our earlier work we assume that the palladium atoms fully occupy their positions in an FCC lattice, and that the conversion to superabundant vacancies has not yet occurred. This assumption impacts only the part of the phase diagram at very high loading; and is relevant to the majority of experiments in which either the temperature is too low for Pd self-diffusion, or else the loading is too low to stabilize vacancies at elevated temperature.

For PdH_x we developed statistical mechanics models based on a generalization of Lacher's model [13] to include O-site and T-site occupation. Such models might be considered to be (simple) mean-field models, in contrast to more sophisticated models that have been published in recent years. Instead of making use of isotherm data to optimize a physical underlying model Hamiltonian, we were interested in the development of a simpler empirical mean-field model that might provide for a statistical mechanics engine that we could use for estimating the hydrogen chemical potential at different temperatures and loadings in numerical simulations.

We have been interested in extending our statistical mechanics models for PdH_x to PdD_x for some time. In this brief report we summarize some of our recent efforts to this end. The first issue to deal with is that the published isotherms are generally not particularly consistent, so that assembling a suitable phase diagram for PdD_x from experimental data is problematic. In response we selected a subset of the available data minimally inconsistent to work with. We made

use once again of an extrapolation to low loading as in the case of the PdH_x phase diagram. For PdD_x this seems to work well enough. At high loading we initially attempted to extrapolate as before; however, this time the data sets do not extend as far and we were not able to develop reliable extrapolations. We tried developing phase diagram models based on high pressure data only for the lowest temperature used; however, the optimization of the fitting coefficients tended to produce natural extrapolations to high temperature which did not seem particularly physical. In the end what seemed most plausible was to provide a single "guiding" point at high pressure and high loading which resulted in O-site energy curves free of "pinching" or large dispersal near a loading of unity. As a result, the parameterized isotherms that result are "reasonable" at high loading and high temperature within the framework of the model, and not informed by experimental data. In essence the phase diagram model by itself provides for an extrapolation to high loading at high temperature. This underscores the need for new experimental measurements of isotherms in this regime.

Given that extrapolations to high loading are problematic, especially at high temperature, we were motivated to revisit the phase diagram for PdH_x and develop an analogous phase diagram model free of such extrapolations. Once again a single "guiding" point at high pressure and high loading is used to constrain the phase diagram and O-site energies at high loading and at high temperature to be "reasonable".

2. Isotherms

Studies of isotherms with experimental data for PdD_x appear in Refs. [3,14–27]. We made use of the online WebPlotDigitizer of Ankit Rohatgi to develop numerical versions of isotherms from published plots. (Note that in some cases the available online versions of the experimental papers contain plots that are neither precisely vertical nor rectangular, so that some effort was needed to assemble numerical isotherm data.) It became clear from digitizing and comparing isotherms from different references that there were issues with consistency. In some cases isotherms taken at different temperatures would cross, and in other cases isotherms taken at the same temperature would be significantly offset in pressure. The construction of a phase diagram directly from data sets from many groups as was done for PdH_x [28] does not work as well for PdD_x.

2.1. Choice of isotherms

After numerous tries with different isotherm data sets, in the end we decided to work with: the 298 and 323 K isotherms of Sakamoto et al. (1996) [25]; the 348 K isotherm of Kibria et al. (1998) [26]; and the set of isotherms at 393, 433, 473, 533, 573, and 613 K of Wicke and Blaurock (1987) [22]. We note that the 348 K isotherm of Kibria et al. does not seem to be particularly consistent with the data sets of Sakamoto et al. or of Wicke and Blaurock. Even so, this choice of isotherms seemed better than other sets that we worked with earlier in the study.

2.2. Extrapolation to low loading

In order to construct a model phase diagram along the lines discussed in previous publications, we need to extrapolate the isotherms down to lower pressure and loading (which allows us to develop appropriate initial conditions for the fitted isotherms). To do this we made use of extrapolated isotherms based on

$$\ln P(\mathrm{atm}) = \left(\frac{a_{-1}}{T} + a_0 + a_1 T\right) + \left(\frac{b_{-1}}{T} + b_0 + b_1 T\right)\theta + 2\ln\frac{\theta}{1-\theta}. \tag{1}$$

We made use of α-phase isotherm data published by Clewley et al. (1977) [3], Kleppa and Phutela (1982) [18], and by Lasser (1984) [20]. The fitting parameters were optimized to give

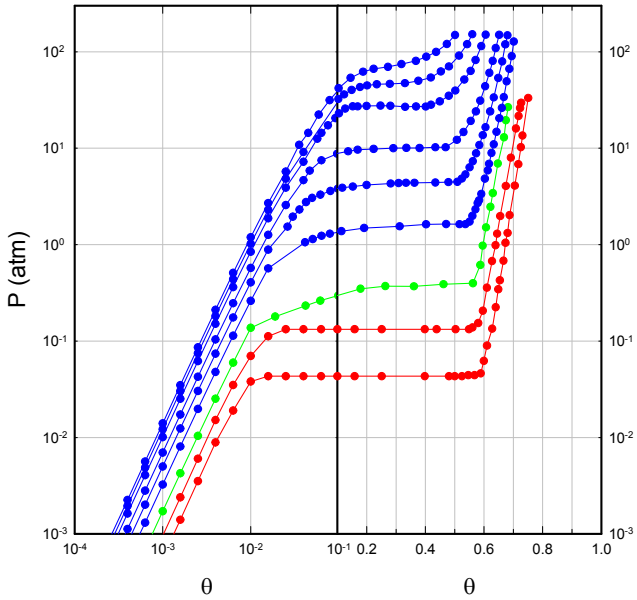

Figure 1. Desorption isotherms extrapolated to lower pressure and loading. The circles indicate the loading and pressure data points digitized from [25] in red, [26] in light green, and from [22] in blue; along with extrapolations of the data into the α-phase.

$$a_{-1} = -2375.64\,\mathrm{K}, \quad a_0 = 15.4305, \quad a_1 = -0.00324156\,\mathrm{K}^{-1},$$
$$b_{-1} = 2034.1\,\mathrm{K}, \quad b_0 = -46.2616, \quad b_1 = 0.0372747\,\mathrm{K}^{-1}, \tag{2}$$

The results are shown in Fig. 1.

2.3. Data points at high loading

In previous work we extrapolated isotherms to higher loading making use of simple extrapolation formulas [10]. As mentioned in the Introduction, we attempted a similar approach with the isotherms under discussion in this section. Unfortunately, in this case there were problems developing a suitable extrapolation (since the PdD $_x$ isotherm data does not go to as high pressure). Instead, it seemed best to make use only of the model results at high loading at 300 K from [5] to serve as an informed extrapolation at room temperature.

3. PdD$_x$ Phase Diagram Model

Our efforts toward developing a model phase diagram for PdH $_x$ included working with numerous different types of models, as discussed in [10]. In the end the results deemed to be best were obtained from a mean field model based on an O-site to T-site energy difference which depends on loading (and not on temperature), and on an O-site energy that depends on both loading and temperature. For the PdD $_x$ phase diagram we decided to optimize a similar model, expecting qualitatively similar results since PdH$_x$ and PdD$_x$ are closely related theoretically.

In the course of our study we developed more than 50 optimizations of a variety of different models (and also with different isotherm data sets). The results obtained for PdD_x were found not to be particularly close to the result obtained previously for PdH_x. This motivated us to develop new optimizations for the PdH_x phase diagram using a similar approach, hoping to resolve the differences. In the end good results were obtained as discussed in Section 3.1.

3.1. Model for the O-site energy

The optimization of a phase diagram model was done following the approach discussed in [10]. For a generalized Lacher type of mean-field model the O-site energy $E_{\rm O}$ is optimized to minimize the difference between the model chemical potential and the chemical potential that corresponds to the experimental isotherm data. For the study reported here we made use of an O-site energy that depends on loading and temperature according to

$$E_{\rm O}(\theta,T)+\frac{E_{\rm D}}{2}=\left[a_0+a_1\theta+a_2\theta^2+a_3\theta^3+a_4\theta^4+a_5\theta^5+a_6\theta^6\right] + T\left[b_0+b_1\theta+b_2\theta^2+b_3\theta^3+b_4\theta^4+b_5\theta^5+b_6\theta^6\right], \tag{3}$$

where $E_{\rm D}$ is the D_2 dissociation energy. This corrects the definition of the parameterization of the O-site energy from [10] (where the $E_{\rm D}/2$ factor was omitted).

3.2. Results

As mentioned in Section 1, what seemed to be the best results were obtained where we allowed the model to fit the experimental and α-phase extrapolated data. However, left to itself the optimization would in some cases produce a pinching or a deviation of the O-site energies at high loading. This provided motivation to introduce a single "guiding" point at high temperature and high pressure to minimize these effects. The fitted phase diagram that results in shown in Fig. 2. One can see two added points near room temperature at high loading consistent with the models discussed in [5], along with a high temperature "guiding" point at high pressure.

The a_j fitting parameters used for the O-site energy are (in meV) are as follows:

$$a_0=-72.435,\quad a_1=-249.999,\quad a_2=87.897,\quad a_3=-39.679,$$

$$a_4=103.705,\quad a_5=230.615,\quad a_6=-214.613, \tag{4}$$

and the b_j fitting parameters are (in meV/K)

$$b_0=0.02810,\quad b_1=0.03778,\quad b_2=0.09514,\quad b_3=-0.15121,$$

$$b_4=-0.01107,\quad b_5=0.00714,\quad b_6=0.03747. \tag{5}$$

The resulting O-site energies are shown in Fig. 3.

4. PdH_x Phase Diagram Model

As discussed above we carried out new optimizations for the PdH_x phase diagram using the same approach hoping for qualitatively similar results in terms of the resulting mean field model. The resulting phase diagram is shown in Fig. 4.

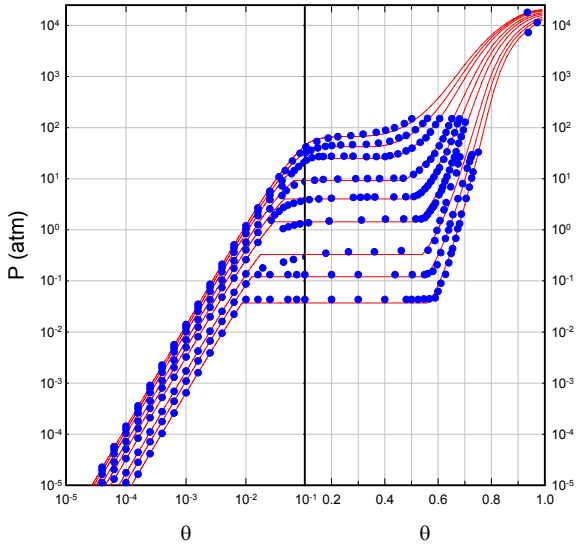

Figure 2. Model isotherms (*red lines*) and input isotherm points (*blue circles*) for PdD_x.

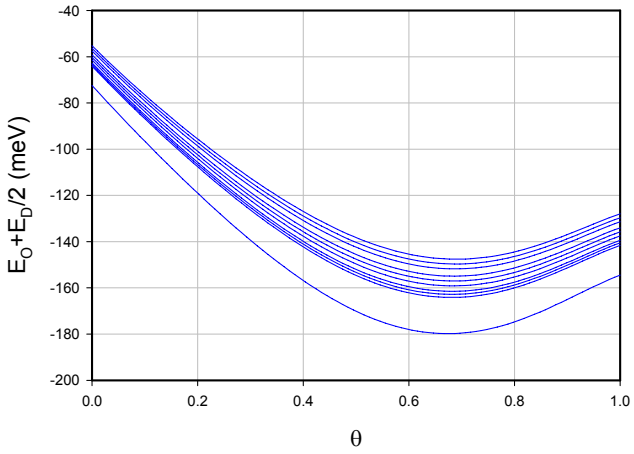

Figure 3. Model O-site energies in meV as a function of loading for (from lowest to highest curves) T = 0,298, 323, 348, 393, 433, 473, 533, 573, and 613 K.

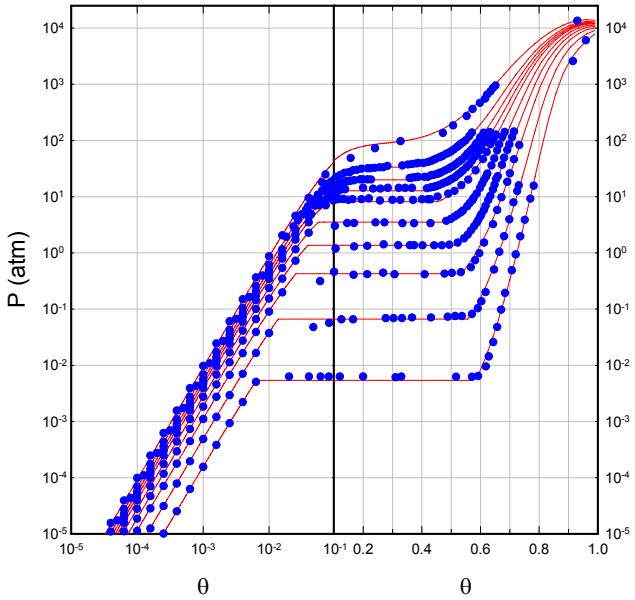

Figure 4. Model isotherms (*red lines*) and input isotherm points (*blue circles*) for PdH_x. The isotherms from lowest to highest correspond to temperatures of for (from lowest to highest curves) $T = 293$, 343, 393, 433, 473, 516, 543, 573, 613, and 710 K.

The a_j fitting parameters obtained in this case (in meV) are

$$a_0 = -74.835, \quad a_1 = -260.600, \quad a_2 = 56.644, \quad a_3 = 15.128,$$
$$a_4 = 78.713, \quad a_5 = 211.893, \quad a_6 = -195.118, \tag{6}$$

and the b_j fitting parameters in (meV/K) are

$$b_0 = 0.02791, \quad b_1 = 0.08690, \quad b_2 = 0.01451, \quad b_3 = -0.07286,$$
$$b_4 = -0.00988, \quad b_5 = 0.00620, \quad b_6 = 0.00635. \tag{7}$$

O-site energies for this model are shown in Fig. 5.

5. Discussion

The general approach discussed in our previous efforts to construct phase diagram models for PdH_x in [10] seems sound (with the exception of making use of extrapolations to fill in where experimental data is lacking at high loading and at high temperature). Consequently, we thought that the extension of the approach to PdD_x should result in a reasonable phase diagram model. The biggest issues we encountered in this project were the selection of isotherm data, and technical issues associated with developing a faithful digitization.

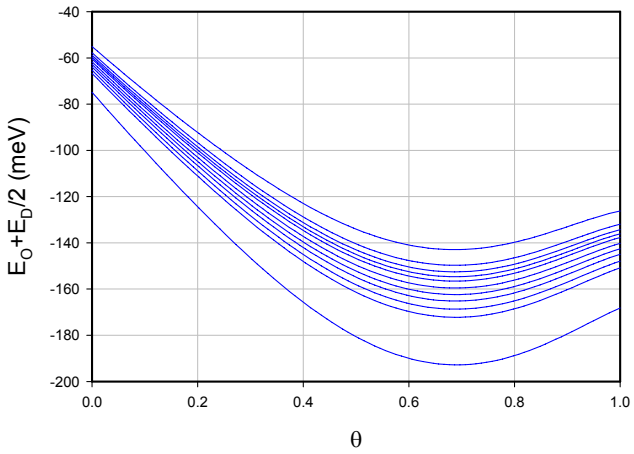

Figure 5. Model O-site energies in meV as a function of loading for (from lowest to highest curves) $T = 0$, 293, 343, 393, 433, 473, 516, 543, 573, 613, and 710 K.

We made use of our earlier work on isotherms at high loading near room temperature [5] to provide estimates for pressure at two loading points for both PdD_x and PdH_x. We tried a variety of "guiding" points at high loading and at high temperature, seeking a "reasonable" solution in both cases. What was found was that if the guiding point was too low, then the $E_{\rm O}$ curves would droop near $\theta = 1$; and if the guiding point was too high then the $E_{\rm O}$ curves began to diverge. Once again, we would prefer to work with experimental data for this region, but as yet none is available.

The phase diagram models that result in both cases match the isotherm data quite well, with unweighted mean square errors I (see [10]) on the order of 2.2×10^{-5} for PdD_x and 1.4×10^{-5} for PdH_x. In our earlier work we appeared to get a spread at low loading that could be interpreted as associated with the shift in the Fermi level, but this effect does not show up in the models and optimization reported on here.

We had expected the O-site energy curves should be similar for the two cases extrapolated to $T = 0$. The agreement is good at low loading, but the PdH_x O-site energy shows a minor deviation, ending up more than 10 meV lower at a loading of unity. This is likely a result of the larger lattice constant for PdH_x as the loading increases. The biggest difference between the two models obvious from the $E_{\rm O}$ vs. θ plots is that there is a larger spread in the $E_{\rm O}$ curves at different temperatures for PDH_x than for PdD_x, which is likely due to the larger number of low-energy configurations available to PdD_x as the loading increases.

Appendix A. Role of Superabundant Vacancy Phases

A reviewer has asked about the role of the superabundant vacancy phase in PdD_x, which is relevant since vacancy phases are preferred thermodynamically at high loading.

People had long modeled solid state systems based on (simple) atom-atom potentials, until the early 1980s when it was observed that embedded atom models that took into account in addition the background electron density could connect with experiment [31]. Following this, embedded atom models were developed for helium and hydrogen in metals and applied systematically to the analysis of light interstitials, as well as for hydrogen and helium in vacancies. Estimates that resulted for the binding energy of H and D in vacancies [32,33] indicated that vacancies are traps for

hydrogen isotopes in Ni and Pd. Two measurements of the monovacancy enthalpy for bulk Pd has been measured giving 1.85 eV [34] and 1.5 eV [35]. If there is an interstitial hydrogen or deuterium in an O-site next to a Pd atom, the vacancy formation energy is reduced by more than 200 meV (and further reduced with more interstitial neighbors). This suggests that at a D/Pd loading near unity the vacancy formation energy will be much reduced, and that vacancies should form spontaneously.

However, the spontaneous formation of superabundant vacancies has not been reported in electrochemical experiments near room temperature. For the lattice to rearrange itself into one of the superabundant vacancy phases, the host Pd atoms need to diffuse to other locations. The atomic self diffusion coefficient for Pd in bulk Pd is very low [36,37], so that a conversion to a vacancy phase would be expected to take a prohibitively large number of years (unless the phase change to a vacancy phase were to proceed like a more conventional rearrangement type of phase change not involving vacancies, but as yet there is not evidence for this). We would expect faster self-diffusion in PdD_x [38–40], but we would not expect the self-diffusion to be sufficiently fast to change the conclusion here. To arrange for a faster conversion, Fukai and Okhuma used an elevated temperature between 700 and 800 °C [11] where the conversion to the vacancy phase took several hours.

Consequently, even though the superabundant vacancy phases are expected to be preferred thermodynamically at high loading, a PdD_x sample would not be expected to convert to the vacancy phase in a relevant time scale (although a focused experimental clarification of this point would be of great interest). Under these conditions the use of a phase diagram based on α-phase, β-phase and miscibility gap region for FCC Pd as presented in this work is relevant and useful.

We have noted previously that special arrangements need to be made in order to develop superabundant vacancies in an electrochemical experiment near room temperature. Since the Pd atoms in the cathode would have a negligible self-diffusion coefficient (and would not be expected to move much), we might consider the addition of new Pd through codeposition as a way to make a vacancy phase layer if the D/Pd loading is sufficiently high when the codeposition occurs. This was offered as an interpretation [41] for the rapid development of excess heat in the Szpak codeposition experiment [42]. Letts demonstrated a prompt excess heat heat following Pd codeposition at high current density [43]. The idea in this experiment is that co-deposition at high current density allows for a high loading near the surface, but the Pd co-deposition rate is kept low by limiting the number of Pd^{2+} ions in the electrolyte in order to allow time for the Pd atoms at the surface to move to locations that minimize energy. Whether superabudant vacancies are produced in the Letts co-deposition experiment has not been clarified experimentally yet.

Appendix B. Partial Enthalpy of Formation

A reviewer wonders about partial enthalpy in the comment:

The data of Flanagan et al. as well as Sakamoto et al. both show that the partial enthalpy of formation of hydrogen becomes endothermic at some composition within the beta phase. This behavior would be expected to cause the log P(H_2) vs, 1/T relationship to change sign at the H/Pd ratio where the exothermic–endothermic transition occurred. This behavior is not included in the evaluation shown here. Why not?

This is an interesting question worth considering. We can write

$$\Delta H = \frac{R}{2}\left(\frac{\partial \ln p}{\partial(1/T)}\right)_\theta \tag{B.1}$$

adapted from Eq. (3.21) in Speiser's review [44]. This in a sense provides a measure of how much change in pressure

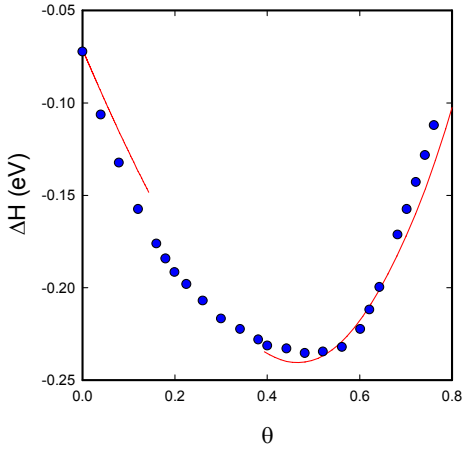

Figure 6. Model partial enthalpy of formation at 590 K (*red line*) as a function of H/Pd outside of the model miscibility gap; partial enthalpy from Flanagan and Luo (*blue points*).

occurs at a specific loading going from an isotherm at one temperature to a nearby isotherm at a slightly different temperature.

In an experiment that focuses on a single isotherm at a single temperature, a determination of ΔH would then allow for an extrapolation to temperatures not measured. It would extend the utility of a single temperature measurement, as well as providing data that can be used to exercise statistical mechanics models.

The same relation can be used to develop systematic estimates for ΔH when a more complete set of data is available; for example as is the case when dealing with the isotherms of a phase diagram. In the model described in this paper, the fitting parameters are optimized so that the model isotherms match the phase diagram data as closely as possible. If the fit is accurate, then we would expect the partial enthalpy to be equivalently accurate.

In response to the reviewer's comment we used the model to calculate ΔH above the critical point for Fig. 1 from Flanagan and Luo [45]. There are technical issues in this comparison, as the model critical point (around 635 K) lies above the critical point experimental from experiment (around 566 K). We compare with a model isotherm calculated at 590 K. The model result outside of the model miscibility gap is in reasonable agreement with the published curve as shown in Fig. 6.

The change in sign of ΔH in this case occurs near $\theta = 0.90$, so the effect of interest in the reviewer's comment is included in the model, although it is a weak effect. One can see a bunching of the isotherms at high temperature and at high loading; which is due primarily to the deviation of the fugacity from the pressure, and in small part from the change in sign of ΔH at high temperature.

Appendix C. Octahedral and Tetrahedral Sites

The reviewer has commented about octahedral and tetrahedral sites:

The H, D atoms in the alpha phase are proposed to occupy random sites located in the interstitial spaces between the Pd atoms. These sites have tetrahedral characteristics. Octahedral sites form only after the Pd atoms shift to form the beta phase. Therefore, the statement that octahedral sites are involved in the evaluation of the alpha phase is

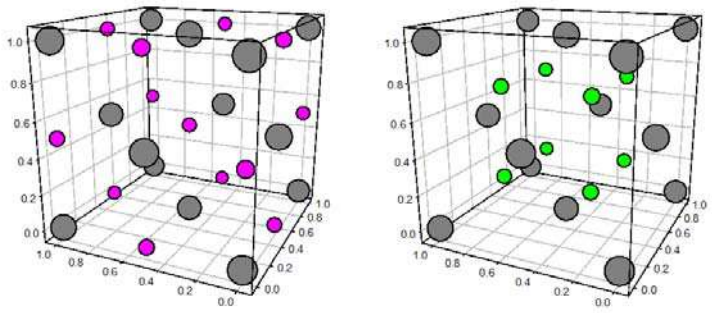

Figure 7. Octahedral (*left*) and tetrahedral (*right*) site locations for interstitial hydrogen isotopes in an FCC metal lattice. The locations of the metal atoms are indicated by the larger gray circles. The O-site positions are indicated by the smaller pink circles on the left; and the T-site positions are indicated by the smaller light green circles on the right.

confusing.

Given the controversy associated with octahedral and tetrahedral site occupation in PdH_x and PdD_x, this issue is one well worth additional discussion.

Appendix C.1. Site locations

Stoichiometric PdH at low temperature is thought to occur in an FCC NaCl type of structure, with the Pd atoms and Pd atoms at alternating positions on a cubic lattice as shown in the left schematic of Fig. 7. The tetrahedral sites occur at interior locations, as indicated in the schematic on the right.

The metal lattice positions in these figures are at

$$\left(0,0,0\right),\left(\frac{1}{2}a,\frac{1}{2}a,0\right)\left(a,0,0\right),\left(0,a,0\right),\cdots$$

and equivalent lattice sites (we have included redundant locations here), where a is the lattice constant. The octahedral sites are located at

$$\left(\frac{1}{2}a,0,0\right),\left(0,\frac{1}{2}a,0\right),\left(0,0,\frac{1}{2}a\right),\left(\frac{1}{2}a,\frac{1}{2}a,\frac{1}{2}a\right),\cdots$$

and equivalent lattice sites (again with redundant locations included). The tetrahedral sites are at

$$\left(\frac{1}{4}a,\frac{1}{4}a,\frac{1}{4}a\right),\left(\frac{3}{4}a,\frac{1}{4}a,\frac{1}{4}a\right),\left(\frac{1}{4}a,\frac{3}{4}a,\frac{1}{4}a\right),\left(\frac{1}{4}a,\frac{1}{4}a,\frac{3}{4}a\right),\left(\frac{3}{4}a,\frac{3}{4}a,\frac{1}{4}a\right),\cdots$$

and equivalent lattice sites (also with redundant locations).

What distinguishes an octahedral site or a tetrahedral site is the position relative to the sites occupied by the metal atoms. There is a single octahedral site in the bulk for each metal atom site, and there are two tetrahedral sites for each metal atom.

Appendix C.2. Site occupation from experiment

The reviewer has suggested that hydrogen and deuterium occupy tetrahedral sites in palladium at low loading in the α-phase, while only at higher loading in the β-phase do octahedral sites form, and that hydrogen and deuterium occupy octahedral sites in the β-phase. In order to make progress on the associated issues we must turn to experiment.

Worsham [46] carried out neutron diffraction experiments at room temperature, and reported that from these experiments octahedral site occupation was dominant in the beta phase for both powder PdH_x and PdD_x. Nelin [47] focused on powder PdH_x and PdD_x at elevated temperature, concluding that hydrogen and deuterium are in octahedral sites, even in the α-phase well above room temperature.

Neutron diffraction works best for this problem when the interstitial occupation is large, which hinders α-phase measurements near room temperature or below. In this case a different approach is required, and ion channeling experiments have proven to be effective. Carstanjen [48] made use of deuterium ion channeling and fusion reactions to determine that deuterium atoms occupy octahedral sites in $PdD_{0.007}$ at low temperature.

Appendix C.3. O-site and T-site occupation in the α-phase

The reviewer has written in addition:

The relationship between O-site and T-site is complex in the alpha phase. Here the O-site is initially much smaller than in the beta phase and, consequently, less likely to be occupied compared to the T-site. Nevertheless, occupancy of the O-site increases with temperature and H/Pd atom ratio, until the alpha and beta phases eventually merge as the temperature is increased above a critical value. Nevertheless, at lower temperatures, this conversion of alpha to beta is a step function with only a very small amount of H in the alpha phase being required to cause the conversion. Once conversion takes place, essentially all of the H in the alpha phase moves to the O sites, thereby causing the lattice to abruptly expand.

Given the prominence of interpretations involving different sites in some of the earlier literature, it seems appropriate to consider this issue here. A comparable picture is described in the case of titanium hydride put forth by E. J. Goon (see the brief discussion in [49]). An early neutron diffraction study in PdH reported different structures at low temperature in β-phase PdH, which was interpreted as due to O-site occupation above 55 K, and a migration to T-site occupation below 55 K [50].

This argument figures prominently in connection with resistance measurements in [51]. Subsequent neutron observations did not confirm the presence of tetrahedral occupation, as discussed in [52,53].

In principle the channeling experiments of Carstanjen should be sufficient to settle the issue. However, attention should be drawn to the measurements of Bugeat and Ligeon, who also observed O-site occupation in Pd loaded in the α-phase by implantation [54]. In this case O-site occupation was observed at low temperature, but when the sample was warmed T-site occupation was observed. The interpretation presented by the authors for this observation was that when the temperature was increased the hydrogen diffused from O-sites to vacancy sites to occupy T-sites. In a monovacancy in Ni (which is similar to the monovacancy in Pd) the O-site lies 3 meV below the T-site [33]. With nearly degenerate O-sites and T-sites in the Pd monovacancy, a more modern interpretation of the Bugeat and Ligeon experiment is that both O-site and T-site occupation of the monovacancies gives rise to some T-site signals.

Note also that while the O-site may be smaller in the α-phase than in the β-phase, the same is true of the T-site. Even so, the associated differences in the zero-point energy much less than the difference that we found for the empirical O-site to T-site excitation energy [5].

So, in this case we are not in agreement with the picture suggested by the reviewer.

References

[1] M. Fleischmann, S. Pons and M. Hawkins, *J. Electroanal. Chem.* **201** (1989) 301; errata **263** (1990) 187.

[2] M. Fleischmann, S. Pons, M.W. Anderson, L.J. Li and M. Hawkins, *J. Electroanal. Chem.* **287** (1990) 293.

[3] J.D. Clewley, T. Curran, T.D. Flanagan and W.A. Oates, Thermodynamic properties of hydrogen and deuterium dissolved in palladium at low concentrations over a wide temperature range, *J. Chem. Soc., Faraday Trans. 1: Phy. Chem. Condensed Phases* **69** (1973) 449–458.

[4] P.L. Hagelstein, O-site and T-site occupation of α–phase PdH_x and PdD_x, *J. Condensed Matter Nucl. Sci.* **17** (2015) 67–90.

[5] P.L. Hagelstein, Empirical models for octahedral and tetrahedral occupation in PdH and in PdD at high loading, *J. Condensed Matter Nucl. Sci.* **17** (2015) 35–66.

[6] B. Baranowski, S.M. Filipek, M. Szustakowski, J. Farny and W. Woryna, Search for cold fusion in some Me–D systems at high pressure of gaseous deuterium, *J. Less Common Metals* **158** (1990) 347–357.

[7] I.F. Silvera and F. Moshary, Deuterated palladium at temperatures from 4.3 to 400 K and pressures to 105 kbar: Search for cold fusion, *Phys. Rev. B* **42** (1990) 9143–9146.

[8] M.C.H. McKubre, The importance of replication, *Proc. ICCF14* (2008) 673–688.

[9] P.L. Hagelstein, Statistical mechanics models for PdH_x and PdD_x, *J. Condensed Matter Nucl. Sci.* **24** (2017) 87–97.

[10] P.L. Hagelstein, Models for the phase diagram of palladium hydride including O-site and T-site occupation, *J. Condensed Matter Nucl. Sci.* **20** (2016) 54–80.

[11] Y. Fukai and N. Okhuma, Evidence of copious vacancy formation in Ni and Pd under a high hydrogen pressure, *Jpn. J. Appl. Phys.* **32** (1993) L1256–L1259.

[12] Y. Fukai and N. Okhuma, Formation of superabundant vacancies in Pd hydride under high hydrogen pressures, *Phys. Rev. Lett.* **73** (1994) 1640–1643.

[13] J.R. Lacher, A theoretical formula for the solubility of hydrogen in palladium, *Proc. Roy. Soc. London, Series A, Math. Phys. Sci.* **161** (1937) 525–545.

[14] L.J. Gillespie and W.R. Downs, The palladium–deuterium equilibrium, *J. Am. Chem. Soc.* **61** (1939) 2496–2502.

[15] T.B. Flanagan, Absorption of deuterium by palladium, *J. Phy. Chem.* **65** (1961) 280–284.

[16] M.J.B. Evans and D.H. Everett, Thermodynamics of the solution of hydrogen and deuterium in palladium, *J. Less Common Metals* **49** (1976) 123–145.

[17] R. Lässer, Palladium–tritium system, *Phys. Rev. B* **26** (1982) 3517–3519.

[18] O.J. Kleppa and R.C. Phutela, A calorimetric-equilibrium study of dilute solutions of hydrogen and deuterium in palladium at 555–909 K, *J. Chem. Phys.* **76** (1982) 1106–1110.

[19] R. Lässer and K.-H. Klatt, Solubility of hydrogen isotopes in palladium, *Phys. Rev. B* **28** (1983) 748–758.

[20] R. Lässer, Solubility of protium, deuterium, and tritium in the α phase of palladium, *Phys. Rev. B* **29** (1984) 4765–4768.

[21] W.A. Oates, R. Lässer, T. Kuji and T.B. Flanagan, The effect of isotopic substitution on the thermodynamic properties of palladium–hydrogen alloys, *J. Phys. Chem. Solids* **47** (1986) 429–434.

[22] E. Wicke and J. Blaurock, New experiments on and interpretations of hysteresis effects of Pd–D_2 and Pd–H_2, *J. Less Common Metals* **130** (1978) 351–363.

[23] D.H.W. Carstens and W.R. David, Equilibrium pressure measurements in the beta region of palladium protide and palladium deuteride, *Los Alamos Report* LA-11456-MS, 1989.

[24] T.B. Flanagan, W. Luo and J.D. Clewley, Calorimetric enthalpies of absorption and desorption of protium and deuterium by palladium, *J. Less Common Metals* **172–174** (1991) 42–45.

[25] Y. Sakamoto, K. Takai, I. Takashima and M. Imada, Electrical resistance measurements as a function of composition of palladium–hydrogen(deuterium) systems by a gas phase method, *J. Phys.: Condensed Matter* **8** (1996) 3399–3411.

[26] A.K.M.F. Kibria, T. Tanaka and Y. Sakamoto, Pressure-composition and electrical resistance-composition isotherms of palladium–deuterium system, *Int. J. Hydrogen Energy* **23** (1998) 891–897.

[27] S.V. Dyomina, M.V. Glagolev and A.I. Vedeneev, Equilibrium pressure over palladium and its alloys, *Int. J. Alternative Energy and Ecology* **S2** (2003) 83–84.

[28] F.D. Manchester, A. San–Martin and J.M. Pitre, The H–Pd (hydrogen–palladium) system, *J. Phase Equilibria* **15** (1994) 62–83.

[29] R. Lässer, Isotope dependence of the phase boundaries in the PdH, PdD and PdT systems, *J. Phys. Chem. Solids* **46** (1985) 33–37.
[30] J.-M. Joubert and S. Thiébaut, Thermodynamic assessment of the Pd–H–D–T system, *J. Nucl. Materials* **395** (2009) 79–88.
[31] N. Esbjerg and J.K. Norskov, Dependence of the He-scattering potential at surfaces on the surface electron-density profile, *Phys. Rev. Lett.* **45** (1980) 807–810.
[32] S. M. Myers, P. Nordlander, F. Besenbacher and J.K. Norskov, Theoretical examination of the trapping of ion-implanted hydrogen in metals, *Phys. Rev. B* **33** (1986) 854–863.
[33] F. Besenbacher, B. Bech Nielsen, J.K. Norskov, S.M. Myers and P. Nordlander, Interaction of hydrogen isotopes with metals: Deuterium trapped at lattice defects in palladium, *J. Fusion Energy* **9** (1990) 257–261.
[34] K. Maier, G. Rein, B. Saile, P. Valenta and H.E. Schaefer, Positron annihilation measurements in Cu, Ni, Pd, and Pt in thermal equilibrium, *Proc. Fifth Int. Conf. on Positron Annihilation*, Sendai, R.R. Hasiguti and K. Fujiwara (Eds.), 1979.
[35] V.E. Zinovev, R.P. Krentsis and P.V. Geld, Thermal diffusivity and thermal conductivity of palladium at high temperatures, *Sov. Phys. Solid State* **11** (1969) 685–687.
[36] N. L. Peterson, Isotope effect in self-diffusion in palladium, *Phys. Rev.* **136** (1964) A568-A574.
[37] J.B. Adams, S.M. Foiles and W.G. Wolfer, Self-diffusion and impurity diffusion of fee metals using the five-frequency model and the embedded atom method, *J. Materials Res.* **4** (1989) 102–112.
[38] R.B. MacLellan, The kinetic and thermodynamic effects of vacancy interstitial interactions in Pd–H solutions, *Acta Materialia* **45** (1997) 1995–2000.
[39] Y. Fukai, The structure and phase diagram of M–H systems at high chemical potentials – High pressure and electrochemical synthesis, *J. Alloys and Compounds* **404–406** (1995) 7–15.
[40] Y. Fukai, Hydrogen induced enhancement of atomic diffusion in metals, *Defect Diffusion Forum* **297–301** (2010) 132–141.
[41] P.L. Hagelstein, Bird's eye view of phonon models for excess heat in the Fleischmann–Pons experiment, *J. Condensed Matter Nucl. Sci.* **6** (2012) 169–180.
[42] S. Szpak, P.A. Mosier-Boss and J.J. Smith, On the behavior of Pd deposited in the presence of evolving deuterium, *J. Electroanal. Chem.* **302** (1991) 255–260.
[43] D. Letts and P.L. Hagelstein *J. Condensed Matter Nucl. Sci.* **6** (2012) 44–54.
[44] R. Speiser, The thermodynamics of hydrogen in metals, *Metal Hydrides*, W. M. Mueller, J. P. Blackledge, and G. G. Libowitz (Eds.), Academic Press, New York, 1968.
[45] T.B. Flanagan and S. Luo, Thermodynamics of hydrogen solution and hydride formation in binary Pd alloys, *J. Phase Equilibria and Diffusion* **28** (2007) 49–57.
[46] J.E. Worsham Jr., M.K. Wilkinson and C.G. Shull, Neutron-diffraction observations on the palladium–hydrogen and palladium–deuterium systems, *J. Phys. Chem. Solids* **3** (1957) 303–310.
[47] G. Nelin, A neutron diffraction study of palladium hydride, *Phys. Stat. Sol. (b)* **45** (1971) 527–536.
[48] H.D. Carstanjen, J. Dünstl, G. Löbl and R. Sizmann, Lattice location and determination of thermal amplitudes of deuterium in α-$PdD_{0.007}$ by channeling, *Phys. Stat. Sol. (a)* **45** (1978) 529–536.
[49] G.G. Libowitz, The nature and properties of transition metal hydrides, *J. Nuclear Materials* **2** (1960) 1–22.
[50] G.A. Ferguson, Jr., A.I. Schindler, T. Tanaka and T. Morita, *Phys. Rev.* **137** (1965) A483–A487.
[51] G. Bambakidis, R.J. Smith and D.A. Otterson, Electrical conductivity versus deuterium concentration in palladium, *Phys. Rev.* **177** (1969) 1044–1048.
[52] J.K. Jacobs and F.D. Manchester, Thermal and motional aspects of the 50 K transition in PdH and PdD, *J. Less Common Metals* **49** (1976) 67–73.

[53] H.W. King and F.D. Manchester, A low-temperature X-ray diffraction study of Pd and some PdH alloys, *J. Phys. F: Metal Phys.* **8** (1978) 15–26.
[54] J.P. Bugeat and E. Ligeon, Lattice location and trapping of hydrogen implanted in FCC metals, *Phys. Lett.* **71A** (1979) 93–96.